WORLD CONFERENCE ON TIMBER ENGINEERING 2025
BRISBANE, AUSTRALIA
Advancing Timber for the Future Built Environment

A DESIGN MODEL FOR CROSS-LAMINATED TIMBER SHEAR WALLS WITH SINGLE CUT-OUT DOOR OPENINGS

Giuseppe D'Arenzo[1], Riccardo Fanti[2], Daniele Casagrande[3], Werner Seim[4], Ghasan Doudak[5]

ABSTRACT: This paper presents an analytical model for the design and verification of monolithic cross-laminated timber (CLT) shear walls with single cut-out door openings. The model accounts for both one and two centers of rotation kinematic behaviours, enabling the prediction of lateral stiffness, internal forces, and elastic load capacity. Formulations are provided for estimating displacements and stress distributions in the lintel and uplift displacement and forces in the hold-downs. Validation against experimental data demonstrates the model's accuracy in predicting elastic response and its conservative estimation of load-carrying capacity. The proposed approach offers a practical tool for engineers, particularly in seismic applications where accurate stiffness and failure prediction are essential.

KEYWORDS: CLT, Shear Walls, Openings, Structural Design, Lateral Behaviour

1 – INTRODUCTION

Cross-laminated timber (CLT) has gained recognition as a sustainable and structurally efficient material for modern construction. Its versatility enables various construction configurations, including platform and balloon-type structures, as well as hybrid systems incorporating reinforced concrete and steel elements. Regardless of the system adopted, the lateral behaviour of CLT buildings is primarily governed by mechanical connections, such as dowel-type fasteners, hold-downs, and angle brackets [1], [2]. In platform-type CLT buildings, shear walls provide lateral resistance, but their structural performance is significantly affected by the presence of openings such as doors and windows [3].

Openings in CLT shear walls can be introduced in two ways: (i) cutting them directly from monolithic CLT panels or (ii) assembling separate CLT elements (i.e., lintel beam and wall segments) using mechanical fasteners. Introducing openings in monolithic shear walls modifies the load transfer mechanism, inducing stress concentrations around openings and potentially leading to brittle failure at the corners of the openings [4]. Additionally, the structural continuity, through lintel beams and parapets, could modify the kinematic behaviour of shear walls, resulting in one or two centers of rotation.

Experimental and numerical studies have shown that shear walls with cut-out openings exhibit higher stiffness and strength than those with mechanically assembled lintels and parapets, yet current design methodologies often neglect to take this behaviour into consideration [5], [6]. Consequently, monolithic shear walls with openings are frequently modeled as segmented shear walls, represented as a cantilever beam, leading to inaccuracies in predicting lateral stiffness, elastic displacements, and failure mechanisms. This is particularly relevant in seismic design, where an accurate assessment of stiffness, kinematic mechanisms, and potential brittle failure is crucial for ensuring ductile energy dissipation in the connections.

Research on CLT shear walls with openings remains limited, but experimental studies have identified key failure mechanisms, including those involving hold-downs and crack propagation at the corners of openings [7]. Numerical models have attempted to capture these behaviours using finite element (FE) methods [8], macro-element frame models [9], and equivalent frame approaches [10]. While many of these modeling techniques have proven effective in predicting the lateral

[1] Giuseppe D'Arenzo, Department of Engineering and Architecture, University of Enna Kore, Enna, Italy;

[2] Riccardo Fanti, Institute of Bioeconomy, National Research Council of Italy, San Michele all'Adige, Trento, Italy

[3] Daniele Casagrande, Department of Civil, Environmental and Mechanical Engineering, University of Trento, Trento, Italy

[4] Werner Seim, Chair of Timber Structures and Building Rehabilitation, University of Kassel, Kassel, Germany

[5] Ghasan Doudak, Faculty of Civil Engineering, University of Ottawa, Ottawa, Canada

 https://doi.org/10.52202/080513-0381

behaviour of CLT shear walls with openings, their applicability in design practice remains limited.

To address these limitations, the current study presents an analytical model aimed at predicting the stiffness and elastic resistance of monolithic CLT shear walls with single door opening. The model builds upon analytical formulations presented in the literature [11], incorporating mathematical expressions for the calculation of lateral stiffness and kinematic behaviour. These formulations are extended to evaluate internal forces in the lintel and the uplift force in the hold-downs, thereby enabling the calculation of shear wall resistance, the prediction of failure mechanisms, and the design and verification of CLT shear walls with openings. The proposed model provides a simple framework for assessing these structural systems, offering engineers a reliable tool for design and verification, particularly in seismic applications, where brittle failure must be avoided.

2 – ANALYTICAL FRAMEWORK FOR LATERAL RESPONSE

The analytical model proposed in [11] enables the calculation of the elastic lateral response of a monolithic CLT shear wall with single openings, applicable to both one and two centre of rotation scenarios (*Figure 1*). Specifically, the model enables the calculation of the shear wall's lateral displacement, uplift displacement and corresponding vertical reactions in the hold-downs, rotation of the wall segments, and the transversal displacement of the lintel. The model assumes elastic behaviour for the lintel and wall base connections, while a rigid behaviour is assumed for the wall segments.

In the following, the equations for calculating displacements, rotations, and transversal deformation of the lintel are reported for both one center of rotation (1CoR) and two centers of rotation (2CoR) cases. The following analysis considers a shear wall with a door opening, while the influence of vertical loads is neglected.

2.1 LATERAL RESPONSE WITH ONE CENTER OF ROTATION (1COR)

In the case of kinematic behaviour with 1CoR, the rotation and uplift of the wall can be calculated with (1) and (2), respectively, where the symbols are defined in *Figure 1*.

$$\theta = F \cdot h_w \frac{k_{HD1-A} + k_B + k_{HD1-B}}{DEN} \tag{1}$$

$$v_1 = F \cdot h_w \frac{k_B(b_{w2} + l_{op}) - k_{HD1-A} \cdot b_{w1}}{DEN} \tag{2}$$

k_B is the elastic transversal stiffness of the beam representing the lintel, which can be calculated with (3). Here, the term β accounts for the shear deformation of the beam, according to Timoshenko's theory, and can be calculated with (4) and (5), in which $EI_{ef,x}$ and $G_{ef}A_s$ represent the effective bending and shear stiffness of the beams, respectively.

The denominator DEN in (1) and (2) can be calculated with (6), whereas the transversal displacement of the lintel can be calculated with (7).

$$k_B = \frac{12EI_{ef,x}}{{l_{op}}^3}\beta \tag{3}$$

2.2 LATERAL RESPONSE WITH TWO CENTERS OF ROTATION (2CORS)

In the case of kinematic behaviour with 2CoRs, the wall rototation can be calculated with (8), where the parameters are defined in *Figure 1*. The transversal displacement of the lintel can be calculated with (9).

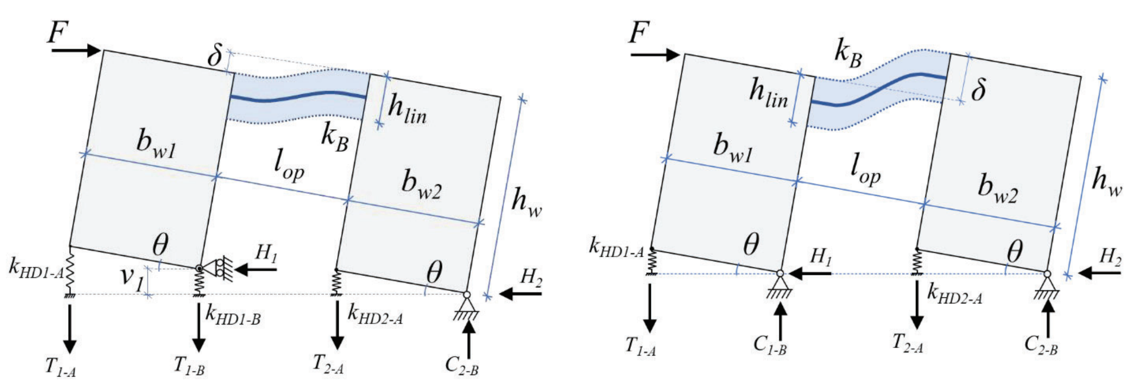

Figure 1. Analytical model: kinematic behaviour with one (a) and two (b) centres of rotation.

https://doi.org/10.52202/080513-0381

$$\beta = \frac{1}{1 + 12 \cdot \alpha} \quad (4)$$

$$\alpha = \frac{EI_{ef,x}}{G_{ef} A_s \cdot {l_{op}}^2} \quad (5)$$

$$DEN = k_{HD1-A} \cdot \left(k_{HD1-B} \cdot {b_{w1}}^2 + k_{HD2-A} \cdot {b_{w2}}^2\right) + k_{HD1-B} \cdot k_{HD2-A} \cdot {b_{w2}}^2 + \\ + k_B \left(k_{HD1-A}\left(b_{w1} + b_{w2} + l_{op}\right)^2 + k_{HD1-B} \cdot \left(b_{w2} + l_{op}\right)^2 + k_{HD2-A} \cdot {b_{w2}}^2\right) \quad (6)$$

$$\delta = \theta\left(b_{w2} + l_{op}\right) - v_1 \quad (7)$$

$$\theta = \frac{F \cdot h_w}{k_{HD1-A} \cdot {b_{w1}}^2 + k_{HD2-A} \cdot {b_{w2}}^2 + k_B \cdot \left(b_{w2} + l_{op}\right)^2} \quad (8)$$

$$\delta = \theta\left(b_{w2} + l_{op}\right) \quad (9)$$

3 – EXTENDED ANALYTICAL MODEL FOR INTERNAL FORCES AND STRESSES

3.1 CALCULATION OF INTERNAL FORCES

The transversal displacement of the lintel can be employed to determine its internal actions, under the assumption that the lintel behaves as an elastic beam (*Figure 1*).

The shear force and bending moment at the end of the lintel can thus be calculated as a function of the trasversal deformation using (10) and (11), respectively.

$$V = \frac{12\, EI_{ef,x}}{l_{op}^3} \cdot \delta \quad (10)$$

$$M = \frac{6\, EI_{ef,x}}{l_{op}^2} \cdot \delta \quad (11)$$

The tensile force in the hold-down of the right wall segment in *Figure 1 (a)* can be calculated with (12).

$$T_{2-A} = k_{HD,2-A} \cdot \theta \cdot b_2 \quad (12)$$

The compressive force at the corner of the right wall segment in *Figure 1 (a)* can be calculated with (13), based on force equilibrium in the vertical direction (*Figure 2*).

$$C_{2-B} = T_{2-A} + V \quad (13)$$

The compression force in the lintel can be calculated with (14), based on moment equilibrium of the right wall segment according to *Figure 2*.

$$N = \frac{M + C_{2-B} \cdot b_2}{h} \quad (14)$$

https://doi.org/10.52202/080513-0381

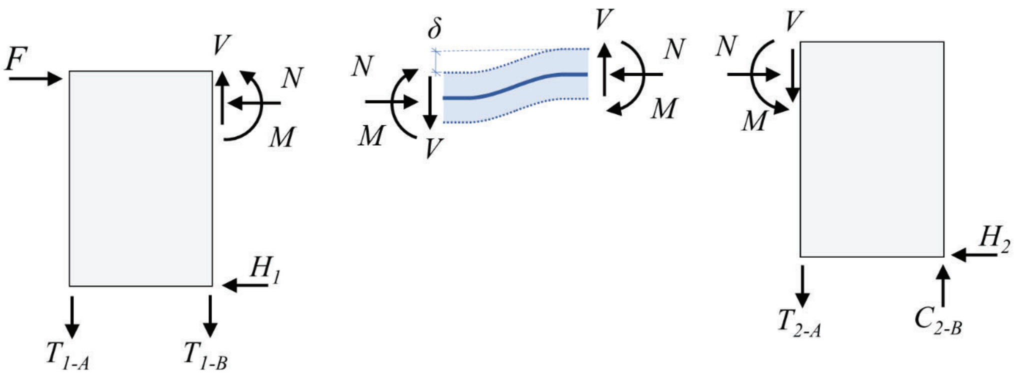

(a)

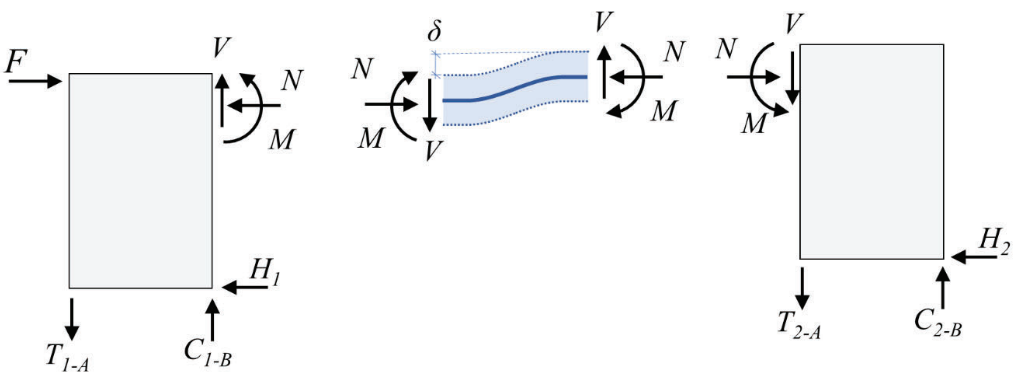

(b)

Figure 2. Internal and external forces in the wall segments and the lintel for the kinematic behaviour with one (a) and two (b) centres of rotation.

The horizontal force at the base of the left and right wall segments can thus be calculated with (15) and (16), based on force equilibrium in the horizontal direction.

$$H_1 = F - N \tag{15}$$

$$H_2 = N \tag{16}$$

The tensile force of the left wall segment according to *Figure 1 (a)* depends on the kinematic behaviour of the shear wall. In the case of 1CoR, it can be calculated with (17), whereas in the case of 2CoRs it can be obtained with (18).

(1CoR) $$T_{1-A} = k_{HD,1-A} \cdot (\theta \cdot b_1 + v_1) \tag{17}$$

(2CoR) $$T_{1-A} = k_{HD,1-A} \cdot (\theta \cdot b_1) \tag{18}$$

3.2 Evaluation of Stresses in the Lintel

The stresses at the ends of the lintel can be calculated based on normal force, shear force and bending moment. A linear distribution can be assumed for the normal stresses at the ends of the lintel, similar to beam theory ([12], [13]). Therefore, the maximum normal stress can be calculated with (19), where $A_{ef,x}$ represents the effective area of the lintel considering the horizontal lamination (20) and $I_{ef,x}$ is the effective moment of inertia (21).

The term t_x in (20) and (21) represents the sum of the thicknesses of the horizontal lamination of the lintel.

$$\sigma_{x,max} = \frac{N}{A_{ef,x}} + \frac{M}{I_{ef,x}} \cdot \frac{h_{lin}}{2} \tag{19}$$

$$A_{ef,x} = t_x \cdot h_{lin} \tag{20}$$

https://doi.org/10.52202/080513-0381

$$I_{ef,x} = \frac{t_x \cdot h_{lin}^3}{12} \tag{21}$$

According to Casagrande et al. [12], a linear distribution can be assumed for the shear stresses at the ends of the lintel, which deviate from the beam theory, where a parabolic distribution is considered. Therefore, the maximum net shear stress can be calculated with (22), where $A_{ef,y}$ is the effective area of the lintel considering the vertical lamination and η is a factor determinaed by Casagrande et al. [12] to calculate the maximum net shear stress at the end of the lintel (23). It is noteworthy to mention that in the case of beam theory η=1.5.

$$\tau_{xy,max} = \eta \cdot \frac{V}{min(A_{ef,x}; A_{ef,y})} \tag{22}$$

$$\eta = \left(1.3 + 0.6\frac{l_{op}}{h_w - h_{lin}}\right) \tag{23}$$

Due to the multi-layered structure of CLT panels, the resisting mechanism for shear forces involves not only net shear stresses but also tangential stresses at the interface between the perpendicular boards of the CLT panel [13], [14], [15]. These tangential stresses can be calculated with (24), where M_{tor} is the torsional moment generated by the tangential stresses (25), I_p is the polar inertia of the resisting interface between the perpendicular boards of the CLT (26), w is the width of the boards, and n is the number of layers in the CLT element.

$$\tau_{tor,max} = \frac{M_{tor}}{I_p} \cdot \frac{w}{2} \cdot \frac{1}{n-1} \tag{24}$$

$$M_{tor} = \tau_{xy,max} \cdot t_x \cdot w^2 \tag{25}$$

$$I_p = \frac{w^4}{6} \tag{26}$$

3.3 VERIFICATIONS

According to several studies in literature [3], [7], the failure mechanism of a monolithic shear wall with opening occur either at the ends of the lintels or in the hold-downs. Therefore, the verifications can be conducted considering the stress state at the ends of the lintel, the tensile force in the most loaded hold-down, and the corresponding material and connection strengths at these locations.

The verifications at lintel ends can be carried out considering the maximum stresses and the corresponding material strengths with (27), (28), and (29), where f_m, f_v, and f_{tor} represent the bending strength, the shear strength related to the net cross section, and the torsional shear strength of the CLT panel, respectively.

$$\frac{\sigma_{x,max}}{f_m} < 1 \tag{27}$$

$$\frac{\tau_{xy,max}}{f_v} < 1 \tag{28}$$

$$\frac{\tau_{tor,max}}{f_{tor}} < 1 \tag{29}$$

In the case of kinematic behaviour with 1CoR, the hold-down subjected to the highest tensile force is that on the left side of the left panel according to *Figure 1 (a)*, whereas, in the case of kinematic behaviour with 2CoRs, the two hold-downs under tension are subjected to the same force. Therefore, the verification in the hold-down can be conducted with (30), where R_{HD} is the tensile capacity of the hold-down.

$$\frac{T_{1-A}}{R_{HD}} < 1 \tag{30}$$

4 – MODEL VALIDATION AGAINST EXPERIMENTAL DATA

This section presents the validation of the analytical model using experimental results. For this purpose, the experimental tests on CLT shear walls with door openings,

https://doi.org/10.52202/080513-0381

Table 1: Geometrical and mechanical properties of the shear walls with door openings tested in Casagrande et al. [7].

ID	h_w	b_w	t_w	h_{lin}	l_{op}	k_{HD}	$E_{ef,v}$	G_{ef}	HD
	[mm]	[mm]	[mm]	[mm]	[mm]	[kN/mm]	[MPa]	[MPa]	conf.
Wall 1	2380	1350	90	340	600	12.3	8940	494	SHD
Wall 2		1200	100	340	900		8327	578	DHD
Wall 4		1200	90	510	1500		8940	494	DHD
Wall 5		1200	100	340	1500		8327	578	DHD

conducted by Casagrande et al. [7], were considered. In the referenced study, four shear walls with different wall segment geometries, lintel configurations, and hold-down arrangements were tested under horizontal loads. The geometrical properties of the walls and the elastic parameters of the hold-downs and CLT panels are summarised in *Table 1*, where t_w represents the thickness of the wall, $E_{ef,v}$ is the effective elastic modulus in the vertical direction of the wall (i.e., aligned with the grain direction of the vertically oriented laminations), G_{ef} is effective in-plane shear modulus of the CLT panel, and the terms SHD and DHD refer to the single and double hold-down configurations, respectively, as defined in [7].

The validation was performed by comparing the experimental load-displacement curves obtained from [7] with those predicted by the analytical model developed in this study. A linear trend was assumed for the analytical load-displacement response, in accordance with the linear elastic assumptions of the model. The load-carrying capacity of the analytical model was identified as the load corresponding to the onset of the first failure, either in the lintel or in the hold-down. This point is determined when one of the ratios (27), (28), or (29) reaches the value of unity. The bending and shear strengths of the CLT lintel were selected based on experimental results obtained from [7], while the torsional strength was chosen according to [10], as reported in *Table 2* and *Table 3*. The hold-down tensile capacity was derived from the experimental results provided by Casagrande et al. [7] (*Table 4*).

The displacement based on the analytical model was calculated as sum of the rocking displacement (31) and panel deformation (32), neglecting the sliding displacement, which is consistent with what was reported in the experimental tests in Casagrande et al. [7]. For the panel deformation, both bending and shear deformation are considered in (32), where I_w is the moment of inertia of the cross-section of the wall-segment.

Table 2: Bending and shear strength of the CLT lintel.

Strengths	for t_w=90 mm	for t_w=100 mm
f_m [N/mm^2]	48.52	50.20
f_v [N/mm^2]	9.08	10.96

Table 3: Torsional strength of the CLT lintel.

f_{tor} [N/mm^2]	3.50

Table 4: Hold-down tensile capacity.

R_{HD} [kN]	94.9

$$\Delta_{rock} = \theta \cdot h_w \tag{31}$$

$$\Delta_{pan} = \frac{1.2 \cdot F/2 \cdot h_w}{G_{ef} \cdot t_w \cdot b_w} + \frac{F/2 \cdot h_w^3}{3 \cdot E_{ef,v} \cdot I_w} \tag{32}$$

Figure 3 shows the comparison between the experimental and analytical load-displacement curves. It can be observed that the analytical model provides an accurate prediction of the elastic stiffness and a reasonable conservative approximation of the load capacity. However, some discrepancies were identified in predicting the failure mode of the shear walls. Specifically, the analytical model consistently predicted failure at the lintel ends, whereas experimental tests on Wall 04 and Wall 05 revealed failure in the hold-downs. This divergence may be attributed to the inherent variability in the mechanical properties of the CLT panels and the connections, as well as the complexity of distinguishing between yielding-type

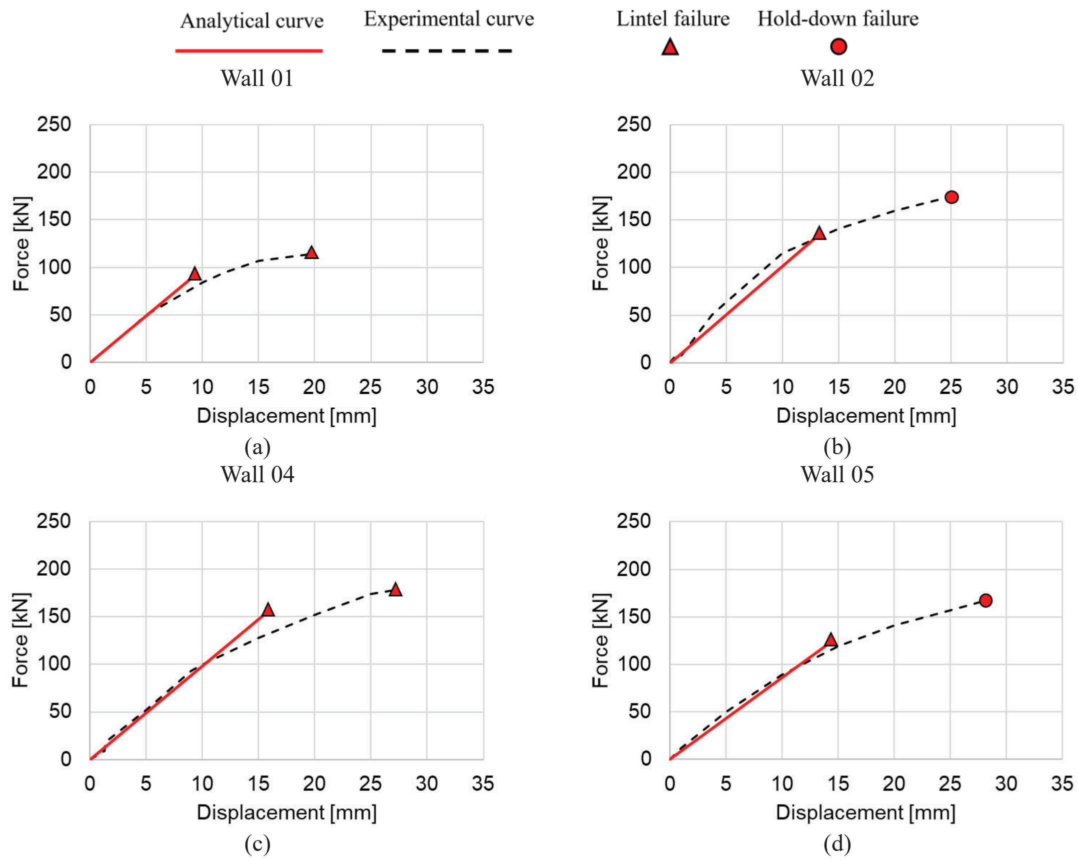

Figure 3. Comparison between the load–displacement curves of analytical model and experimental test.

failures and brittle fracture propagation in real tests. It is also recognised that the actual structural behaviour, especially near failure, may involve fracture initiation and propagation mechanisms that are not fully captured by the analytical model, and that yielding in the hold-downs may have occurred concurrently with or shortly after other damage initiation points. Therefore, while the model provides useful insights for design, it cannot fully replicate the complexity of the observed failure mechanisms.

5 – CONCLUSIONS

This study presented an analytical model for the design and the verification of monolithic CLT shear walls with a single door openings. The model represents an extension of a previously developed analytical model, which provides equations to estimate key parameters of the elastic behaviour such as lateral displacement, wall rotation and uplift, and lintel deformation. The model was formulated for both one center of rotation (1CoR) and two center of rotation (2CoRs) kinematic behaviours, neglecting vertical loads.

The extension of the analytical model allowed for the evaluation of internal forces in the lintel and at the base of the wall panels, and stress distributions in the lintel ends. The proposed verifications were based on stress and force equilibrium conditions, considering compressive, bending, shear, and torsional effects in the lintel as well as tensile forces in the hold-downs.

The model was validated against experimental results from the literature, showing good agreement in predicting elastic stiffness and a conservative estimation of load capacity. However, some discrepancies were observed in the failure mechanisms, as the analytical model systematically predicted lintel failure, while certain experimental tests exhibited failure in hold-downs. These differences may be attributed to the inherent variability in the mechanical properties of the CLT panels and the complex behaviour of the connections, particularly in distinguishing between yielding and brittle failure modes. These findings

https://doi.org/10.52202/080513-0381

highlight the importance of further investigation to improve the reliability of analytical predictions in capturing real structural behaviour.

Overall, the proposed analytical model provides a practical and reliable tool for the design of CLT shear walls with openings, particularly in seismic applications where accurate estimation of stiffness and load capacity is of critical importance. Future developments may aim to incorporate material variability and nonlinear effects in order to enhance the predictive capability of the model.

7 – REFERENCES

[1] C. M. and N. K. A. Ceccotti, C. Sandhaas, M. Okabe, M. Yasomura, "SOFIE project-3D shaking table test on a seven-storey full-scale cross-laminated building," *Earthq. Eng. Struct. Dyn.*, vol. 42, no. 13, pp. 2003–2021, 2013, doi: 10.1002/eqe.

[2] M. Popovski and I. Gavric, "Performance of a 2-Story CLT House Subjected to Lateral Loads," *J. Struct. Eng.*, vol. 142, no. 4, pp. 1–12, 2016, doi: 10.1061/(ASCE)ST.1943-541X.0001315.

[3] B. Dujic, S. Klobcar, and R. Zarnic, "Influence of Openings on Shear Capacity of Wooden Walls," *Proc. 40th CIB-W18 Meet.*, vol. 16, no. 1, pp. 5–17, 2007, [Online]. Available: http://scholar.google.com/scholar?hl=en&btnG=Search&q=intitle:Influence+of+Openings+on+Shear+Capacity+of+Wooden+Walls#0

[4] M. Sciomenta, R. Fanti, G. Doudak, A. Polastri, and D. Casagrande, "Predicting the non-linear behaviour of cross laminated timber shearwalls with cut-out openings," *Structures*, vol. 68, no. June, p. 107138, 2024, doi: 10.1016/j.istruc.2024.107138.

[5] M. Yasumura, K. Kobayashi, M. Okabe, T. Miyake, and K. Matsumoto, "Full-Scale Tests and Numerical Analysis of Low-Rise CLT Structures under Lateral Loading," *J. Struct. Eng. (United States)*, vol. 142, no. 4, pp. 1–12, 2016, doi: 10.1061/(ASCE)ST.1943-541X.0001348.

[6] E. M. Ruggeri, G. D'Arenzo, and M. Fossetti, "Investigating the effect of the structural interactions due to floors and lintels on the lateral response of multi-storey Cross-Laminated Timber shear walls," *Eng. Struct.*, vol. 290, no. April, p. 116327, 2023, doi: 10.1016/j.engstruct.2023.116327.

[7] D. Casagrande, R. Fanti, G. Doudak, and A. Polastri, "Experimental and numerical study on the mechanical behaviour of CLT shearwalls with openings," *Constr. Build. Mater.*, vol. 298, p. 123858, 2021, doi: 10.1016/j.conbuildmat.2021.123858.

[8] M. Mestar, G. Doudak, A. Polastri, and D. Casagrande, "Investigating the kinematic modes of CLT shear-walls with openings," *Eng. Struct.*, no. October, p. 111475, 2020, doi: 10.1016/j.engstruct.2020.111475.

[9] M. Mestar, G. Doudak, M. Caola, and D. Casagrande, "Equivalent-frame model for elastic behaviour of cross-laminated timber walls with openings," *Proc. Inst. Civ. Eng. - Struct. Build.*, vol. 173, no. 5, pp. 363–378, 2020, doi: 10.1680/jstbu.19.00057.

[10] D. Casagrande, G. Doudak, M. Vettori, and R. Fanti, "Proposal for an equivalent frame model for the analysis of multi-storey monolithic CLT shearwalls," *Eng. Struct.*, vol. 245, no. January, p. 112894, 2021, doi: 10.1016/j.engstruct.2021.112894.

[11] G. D'Arenzo, "An elastic model for the prediction of the lateral response of Cross-Laminated Timber shear walls with openings," *Eng. Struct.*, vol. 274, no. September 2022, p. 115055, 2023, doi: 10.1016/j.engstruct.2022.115055.

[12] D. Casagrande, R. Fanti, M. Greco, I. Gavric, and A. Polastri, "On the distribution of internal forces in single-storey CLT symmetric shear-walls with openings," *Structures*, vol. 33, no. May 2020, pp. 4718–4742, 2021, doi: 10.1016/j.istruc.2021.06.084.

[13] H. Danielsson, H. Danielsson, and E. Serrano, "Cross laminated timber at in-plane beam loading – Prediction of shear stresses in crossing areas stresses in crossing areas," *Eng. Struct.*, no. March, pp. 0–1, 2018, doi: 10.1016/j.engstruct.2018.03.018.

[14] W. Seim, *Structural Timber Design*. Ernst & Sohn GmbH, 2024. doi: 10.1002/978343361159.

[15] M. Flaig and H. J. Blaß, "Shear Strength and Shear Stiffness of CLT-Beams Loaded in Plane," *Int. Counc. Res. Innov. Build. Constr. Work. Comm. W18-Timber Struct.*, pp. 243–258, 2013.